27th EPS Conference on Contr. Fusion and Plasma Phys. Budapest, 12-16 June 2000 ECA Vol. **24B** *(2000) 1593 -1596*

Impurity Behavior in MARFE Plasma

K. Shimizu and T. Takizuka

Japan Atomic Energy Research Institute
Naka-machi, Naka-gun Ibaraki-ken, 311-0193, JAPAN

1. Introduction

The high heat load onto divertor plates is one of the most crucial issues for the design of a tokamak fusion reactor. Impurity radiation at the plasma edge and in the divertor region is very effective in reducing this high heat load. However, in discharges with such impurity seeding, the radiation near an X-point is enhanced locally and often leads to a MARFE. We investigate what carbon, e.g., chemically/physically sputtered from wall/target plates, contribute mainly to the radiation near the X-point with a Monte Carlo simulation code, IMPMC [1]. Impurity retention in the divertor region is basically determined by the balance between the thermal force and the friction force. A new expression of thermal force was recently derived in the drift kinetic model [2]. We also discuss about the effect of the kinetic thermal force on the impurity behavior.

2. Simulation model

Simulations of carbon impurity transport have been carried out for a ITER like divertor configuration in size of JT-60U. In Fig.1 we show the non-orthogonal grid used for calculations. The background plasma parameters are calculated with a 2D fluid code SOLDOR [3] coupled with a 2D Monte Carlo neutral code NEUT2D. The model equations used in the SOLDOR code are identical to the B2-code. Fluid equations are discretized in space by a finite volume method (FVM) and are discretized in time with a full implicit manner. The equations are linerlized by the Newton-Raphson method. The discretized equations are solved efficiently using approximate factorization method (AF). The feature of our code is that the total variation diminishing scheme (TVD) is applied for connective terms. The TVD schemes add the minimum dissipation to get a solution without numerical oscillation and can simulate a shock wave without a deformation of shock front.

As for impurity modelling, we adopted Monte Carlo model to take into account kinetic effects. For the thermal force, however, the averaged one over Maxwellian velocity distribution of impurity ions was employed [4]. Using drift kinetic model, a new expression of thermal force was recently derived [2]. In contrast with the averaged thermal force, the kinetic thermal force was found to have opposite direction (towards colder region) for impurity ions with a high velocity. We also derived an expression of the kinetic thermal force in another method and numerically calculated. The ion thermal force is defined by

$$\mathbf{R}_T = \int m_I \mathbf{v}\, C(f_I, \delta f_i)\, d\mathbf{v} = \int \mathbf{F}_T(\mathbf{v})\, f_I(\mathbf{v})\, d\mathbf{v} \qquad (1)$$

where C is the Fokker-Planck collision operator, f_I the distribution function of impurity ions, δf_i the ion distribution function distorted by the ion temperature gradient. Substituting $f_I(\mathbf{v}) = \delta(\mathbf{v} - \mathbf{V}_0)$ into the eq.(1), we calculate the force along the magnetic field acting on a particle with a velocity $\mathbf{V}_0$.

$$F_T^{//}(\mathbf{V}_0) \equiv m_I \int d\mathbf{v}' \delta f_i(\mathbf{v}') \{\Delta v_{//}\}_i = \int d\mathbf{v}' \delta f_i(\mathbf{v}') \left\{ -\frac{4\pi\lambda e^4 Z_I^2}{m_{Ii}} \frac{\mathbf{u}\cdot\mathbf{b}}{u^3} \right\} \qquad (2)$$

where m_{Ii} is the reduced mass, $\mathbf{u} = \mathbf{V}_0 - \mathbf{v}'$, $\mathbf{b}$ the unit vector of the magnetic field. Braginskii derived the distorted distribution function by use of Laguerre polynomials [5].

$$\delta f_i(\mathbf{v}) = \frac{n_i}{\pi^{3/2} v_{th}^3} \exp(-\frac{m_i}{2T_i} v^2) \cdot \tau_i \sum_{n=1}^{N} a_n L_n^{(3/2)}(\frac{m_i}{2T_i} v^2) (\mathbf{v} \cdot \nabla_{//} T_i) \qquad (3)$$

where coefficients a_n are $a_1 = \frac{26895}{17056}, a_2 = \frac{1525}{3198}, a_3 = \frac{35}{533}$. The integration of the equation (2) was carried out numerically by using the Gauss-Legendre integral method. Figure 2 shows the kinetic thermal force acting on a particle with $\alpha = 30\,\mathrm{degree}$, where α is an angle between velocity of a test particle and the magnetic field. It should be noted that the kinetic thermal force strongly depends on the impurity speed, i.e., even the direction of the thermal force changes for impurities with a high velocity of the order of the thermal ion velocity $v_{thi} = (2T_i / m_i)^{1/2}$. The kinetic thermal force derived analytically by D. Reiser et al. [2] is also shown by a broken line. Our result agrees well with their theoretical one.

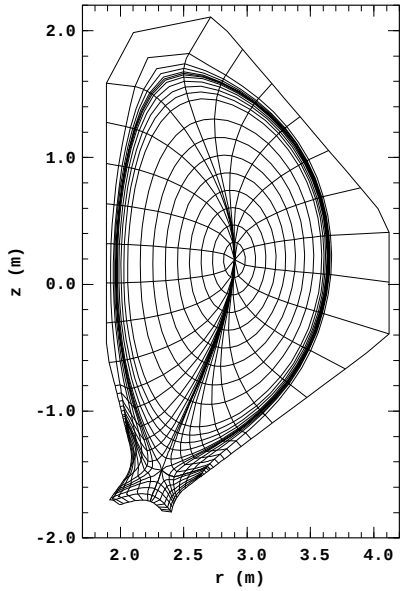

Fig.1 The grid used in simulations. For clarity, some grid points were omitted.

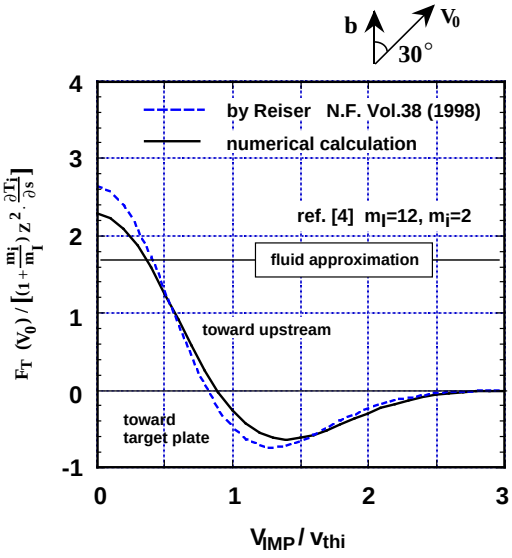

Fig.2 Kinetic thermal force which strongly depends on impurity ion speed Vimp.

3. Background plasma parameters calculated with SOLDOR/NEUT2D

Figure 3 shows the poloidal profile of a detached plasma calculated with the SOLDOR /NEUT2D. The heat flux and the deuterium density on the main plasma boundary are specified, $Q_{tot} = 3$ MW and $n_D = 2.5 \times 10^{19}\,\mathrm{m}^{-3}$, respectively. We use $D_\perp = 0.3\,\mathrm{m}^2/\mathrm{s}$,

$\chi_{\perp}^{i} = \chi_{\perp}^{e} = 1\,\mathrm{m}^2/\mathrm{s}$ as cross filed diffusion coefficients. Taking the impurity effect into consideration, the parallel classical diffusion coefficients are reduced by a factor of 1.8. A simple radiation model is employed, where a fraction of carbon impurity is assumed to be 1.5% of the deuterium density and the radiation loss coefficient is enhanced by impurity transport effect of $n_e \tau_{recycle} = 10^{16}\ \mathrm{s\ m^{-3}}$ [6]. The electron temperature at the divertor plate is reduced to ~1 eV. The peak radiation is located between the target plate and the X-point. Under these plasma parameters of a detached plasma, the impurity behavior is investigated with the IMPMC code. We could not get a steady state owing to the simple radiation model. The X-point MARFE occurred after 1 msec of the plasma shown in Fig.3 and the electron temperature at the X-point was reduced to < 2 eV.

4. Results of IMPMC Simulation

Figure 4 (a) shows the ionization points of physically sputtered carbons. The carbon ionized at the region where T_e is around $\leq \sim 10\,\mathrm{eV}$ and the friction force dominates the thermal force due to short slowing down time. Then most of carbon ions return to the plates. The bolometer tomography data shows that the radiation at the vicinity of the X-point is around $\leq 1\,\mathrm{MW/m^3}$ before an occurrence of X-point MARFE. The calculated carbon density in the main plasma is too low to explain this radiation power. Figure 4 (b) shows the ionization points of chemically sputtered carbons from the private region. The IMPMC code includes the modelling of dissociation process of methane and dynamics of dissociation products (CD_3^+, CD_3, CD_2^+, etc.) In the present calculations, however, we substitute the ionization process of carbon with a low emitted energy (~1 eV) for the complicated processes. The carbon flux chemically sputtered from the wall in the private region is $3.4\times10^{21}\ 1/\mathrm{s}$, using chemical sputtering yield of 0.05. Very few carbons are ionized in the main plasma, as shown in the figure. Therefore, the radiation in the range of MW at the X-point can not be explained. In reality, some of neutral hydrocarbons which can cross the magnetic field enter into the main plasma. Assuming that only 5% of sputtered methane is ionized at the vicinity of the X-point, we calculated the carbon density profiles in the steady state (Fig. 5). We employ $D_{\perp} = 1\,\mathrm{m}^2/\mathrm{s}$ as the diffusion coefficient of carbon ions. The radiation power at the X-point is evaluated: $n_e \cdot n(C^{3+}) \cdot L_z(T_e) = 4.2\times10^{19} \cdot 5\times10^{17} \cdot 10^{-31} = 2\,\mathrm{MW/m^3}$, which is enough to lead an X-point MARFE. Figure 5 also shows comparison of the density calculated with the kinetic thermal force (symbols) and that with the averaged thermal force (solid lines). The difference in the density profiles is very small.

In summary, the chemically sputtered carbons in the private region play an important role on an occurrence of X-point MARFE. The kinetic effect on the thermal force is small in the detached plasma where there is no existence of flow reversal. Our future work is to examine the kinetic thermal force in the detached plasma with flow reversal, or in the X-point MARFE, or for helium as impurity.

Acknowledgments

The authors would like to thank Dr. S. Konoshima for helpful discussions about the radiation profile observed in JT-60U.

References

[1] K. Shimizu, H. Kubo, T. Takizuka et al., J. Nucl. Mater. 220-222 (1995) 410.
[2] D. Reiser, D.Reiter and M.Z. Tokar, Nucl. Fusion 38 (1998) 165.
[3] K. Shimizu, T. Takizuka and T. Hirayama, 41st Annual Meeting of APS, Seattle (1999).
[4] J. Neuhauser, W. Schneider et al., Nucl. Fusion 24 (1984) 39.
[5] S.I. Braginskii, Soviet Phys. JETP 6 (1958) 358.
[6] D.E. Post, J. Nucl. Mater. 220-222 (1995) 143.

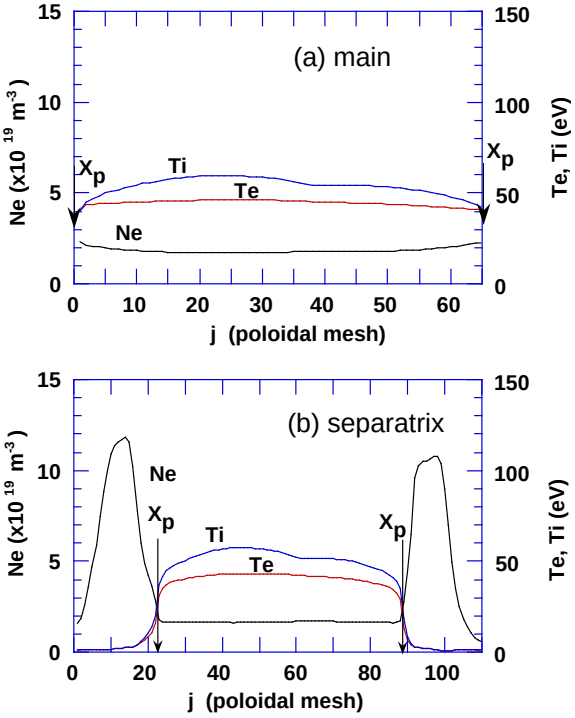

Fig. 3 The poloidal profile of N_D, Ti, and Te used in simulations. (a) in a tube of the main plasma close to separatrix (b) in a tube of SOL close to separatrix.

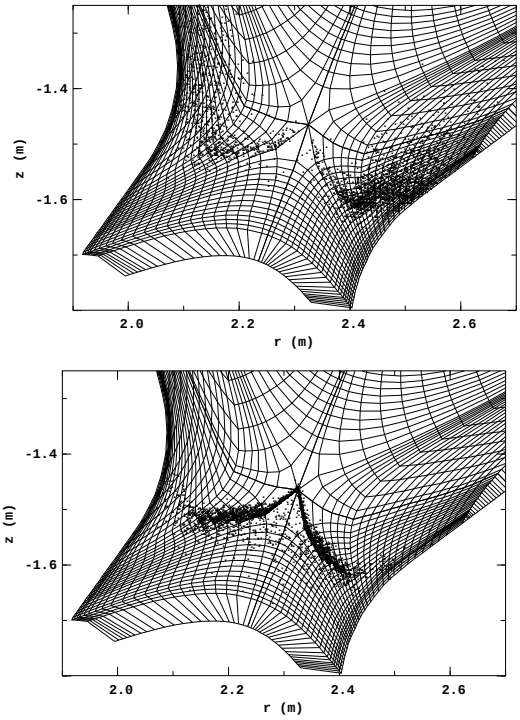

Fig. 4 (a) The ionization points of physically sputtered carbons. (b) The ionization points of chemically sputtered carbons in the private region.

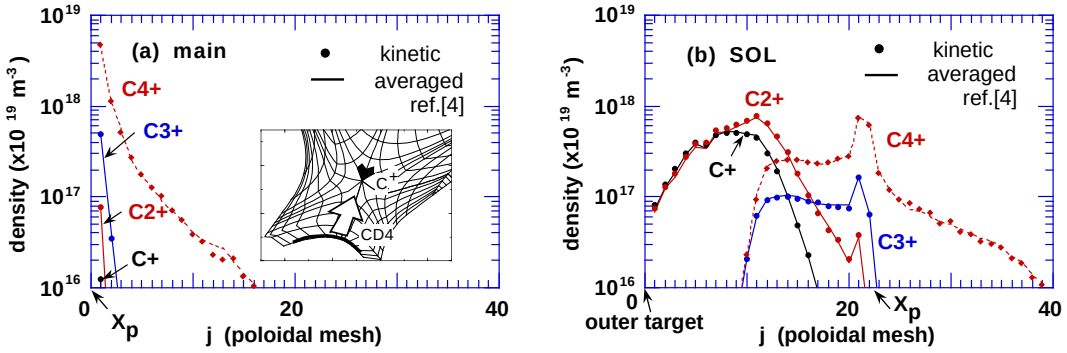

Fig. 5 The carbon impurity density calculated under the assumption that 5% of the methane sputtered from the private region is assumed to be ionized at the vicinity of the X-point shown in a closed polygon region. (a) density profile in the main plasma. (b) the density averaged in the 5 flux tube of the SOL.